

Imaging wound healing using optical coherence tomography and multiphoton microscopy in an *in vitro* skin-equivalent tissue model

Alvin T. Yeh*

Bunsho Kao†

Woong Gyu Jung

Zhongping Chen

J. Stuart Nelson

Bruce J. Tromberg

University of California

Beckman Laser Institute

Laser Microbeam and Medical Program

1002 Health Sciences Road East

Irvine, California 92612

E-mail: ayeh@laser.bli.uci.edu

Abstract. Laser thermal injury and subsequent wound healing in organotypic, skin-equivalent tissue models were monitored using optical coherence tomography (OCT), multiphoton microscopy (MPM), and histopathology. The *in vitro* skin-equivalent raft tissue model was composed of dermis with type I collagen and fibroblast cells and epidermis of differentiated keratinocytes. Noninvasive optical imaging techniques were used for time-dependent, serial measurements of matrix destruction and reconstruction and compared with histopathology. The region of laser thermal injury was clearly delineated in OCT images by low signal intensity. High resolution MPM imaging using second-harmonic generation revealed alterations in collagen microstructure organization with subsequent matrix reconstruction. Fibroblast cell migration in response to injury was monitored by MPM using two-photon excited fluorescence. This study illustrates the complementary features of linear and nonlinear light–tissue interaction in intrinsic signal optical imaging and their use for noninvasive, serial monitoring of wound healing processes in biological tissues.

© 2004 Society of Photo-Optical Instrumentation Engineers. [DOI: 10.1117/1.1648646]

Keywords: optical coherence tomography; multiphoton microscopy; two-photon excited fluorescence; second-harmonic generation; extracellular matrix; tissue engineering.

Paper 014017 received May 19, 2003; revised manuscript received Jul. 15, 2003; accepted for publication Jul. 22, 2003.

1 Introduction

An important feature of high resolution optical imaging technologies such as optical coherence tomography (OCT)¹ and multiphoton microscopy (MPM)² is their capability to image thin sections within thick, living biological tissues nondestructively, without exogenous dyes. This ability has the potential to change the biological paradigm of time-dependent experiments from sequential biopsies using destructive histopathological techniques to serial measurements on the exact same site throughout an extended experimental protocol.

Without the use of exogenous agents, both OCT and MPM rely on spatial inhomogeneities in tissues to provide image contrast. OCT maps the local linear tissue optical scattering properties and MPM relies on differences in the local nonlinear optical properties of tissue. The linear optical scattering properties and nonlinear susceptibilities provide structural and chemical information on the local tissue environment. Characterization of these signals can provide functional information and enhance image contrast.

Herein, thermal injury induced by a Nd:YAP (perovskite) laser in engineered skin-equivalent (raft) tissue models and its subsequent wound healing response were monitored using OCT, MPM, and histopathology. Understanding the wound healing response following laser exposure is essential to en-

hance the therapeutic outcome. *In vitro* skin-equivalent raft tissue models emulate important structural and physiological characteristics of human skin³ and have been shown to respond to both epidermal and dermal injury.^{4,5}

The imaging of burns could find utility in the clinic by diagnosis and noninvasive monitoring of wound healing response after thermal injury. The most important structural component of human skin, collagen,⁶ is also the primary light scattering component.⁷ Thermal injury may perturb the structure of collagen and alter the optical scattering properties of the tissue. By measuring changes in skin light scattering following thermal injury, OCT has shown some success for burn depth analysis.⁸ In tissues with ordered collagen structures, OCT sensitivity to tissue thermal damage can be enhanced using polarization-sensitive detection.⁹ Second-harmonic generation (SHG) has been used for specific imaging of collagen in tissues^{10–12} and has been well characterized.^{13,14} MPM, using SHG, has been shown to be particularly sensitive to the collagen structure.¹⁵ High resolution structural information from MPM is therefore complementary to light scattering measurements of OCT.

High contrast imaging of laser induced thermal injury in skin-equivalent raft tissue models is demonstrated using OCT and MPM. The region of injury is characterized using OCT by significant reduction in light scattering and with MPM by a loss of collagen SHG. Furthermore, high resolution MPM im-

*Current address: Texas A&M University, Department of Biomedical Engineering, College Station, TX 77843.

†Current address: Showa University, School of Medicine, Department of Plastic and Reconstructive Surgery, Tokyo, Japan.

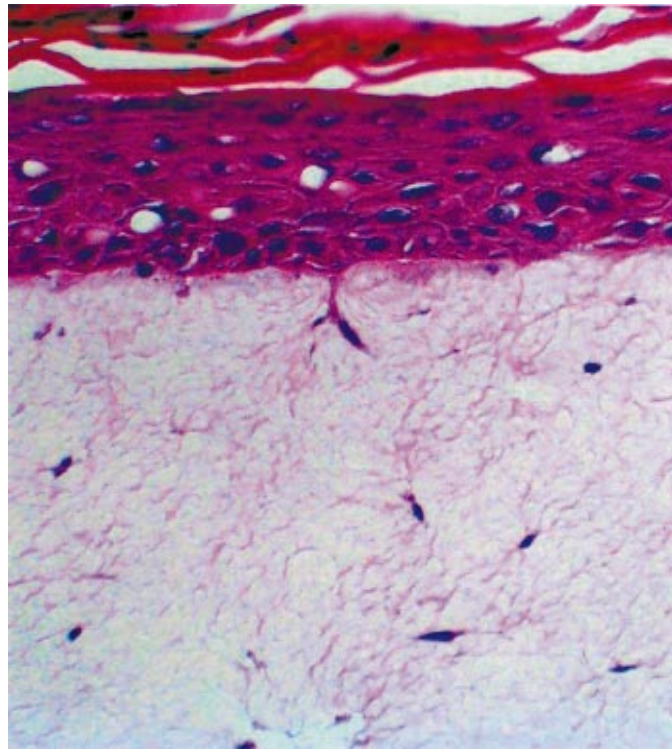


Fig. 1 Image of a 6 μm thick histopathology section of organotypic raft tissue at 20 \times magnification.

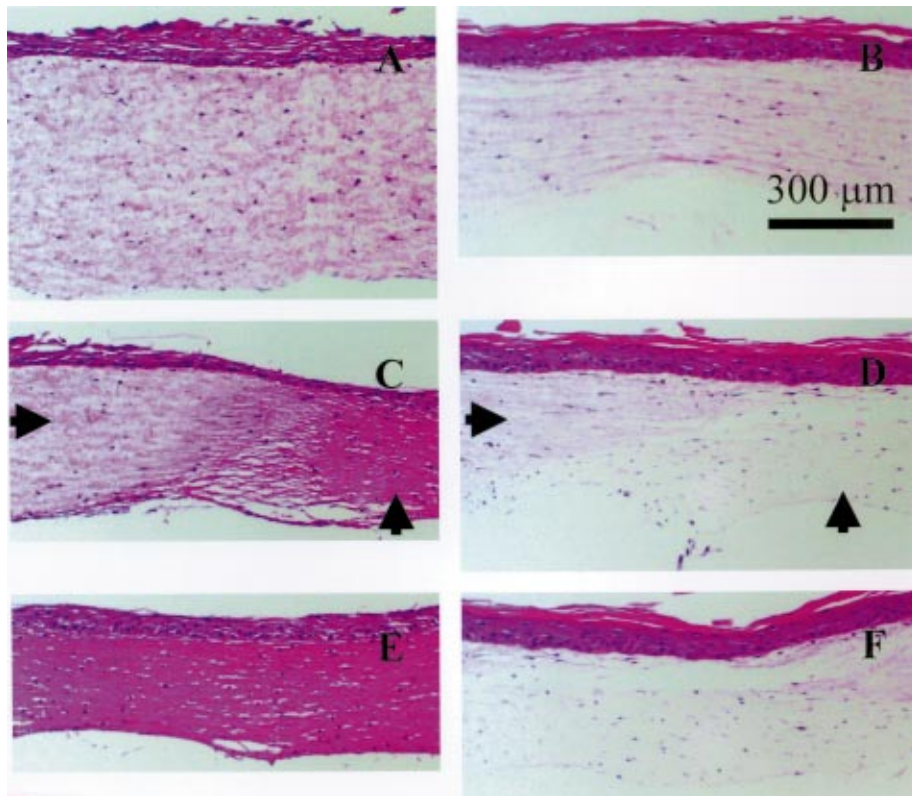


Fig. 2 Histopathology of the raft (A), (C), (E) immediately after laser thermal injury and (B), (D), (F) 10 days thereafter. (A), (B) Nonirradiated regions of the raft. (C), (D) Edge of the laser irradiated region of the raft. Horizontal (vertical) arrows point to the nonirradiated (irradiated) region. (E), (F) Laser irradiated region of the raft.

ages demonstrate that the wound healing process is mediated by infiltration of fibroblast cells into the thermally injured region. Finally, optical imaging of the wound healing response in the raft is compared with histopathology.

2 Experimental Materials and Methods

2.1 Cell Culture

Human epidermal keratinocytes from neonatal skin (Bio Whittaker, Walkersville, MD) were cultured in KGM-2 medium (Bio Whittaker) at 37 °C in 7.5% CO₂ atmosphere. Human dermal fibroblasts were cultured in Dulbecco's modified eagle's medium (DMEM) (Invitrogen, Carlsbad, CA) supplemented with 10% fetal bovine serum (FBS), 20 IU of penicillin/mL, 20 international unit (IU) of streptomycin/mL, and 0.4 mM L glutamine.

2.2 Skin Equivalent (Raft) Tissue Model

Reconstitution buffer was made with 2.2 g NaHCO₃ and 4.77 g HEPES in 100 mL 0.05 M NaOH and sterilized with a 0.22 μm filter. Seven parts of rat-tail collagen, type I (BD Biosciences, Bedford, MA) were mixed with two parts of 5×DMEM and one part buffer and neutralized with 1 M NaOH to pH 7.4±0.2.

Fibroblasts were suspended in the collagen matrix at a density of 4×10⁵ cells/mL. For construction of the dermal layer, 1.5 mL of this suspension was allotted in each well of a 24 well plate (Corning, Corning, NY) and incubated at 37 °C in 7.5% CO₂ atmosphere. Construction of the epidermal layer was initiated 6 h later by suspending keratinocytes in KGM-2 medium at density of 1×10⁶ cells/mL and seeding 0.5 mL aliquots onto each dermal layer of the 24 well plate.

The following day, raft tissues were lifted onto a stainless steel grid support to form an air-liquid interface. Once lifted, keratinocytes and fibroblast cells were nourished by diffusion through the collagen matrix. The keratinocytes were allowed to stratify and differentiate into a 50 μm full-thickness epithelium with 10–12 layers. All raft models were constructed and incubated under identical conditions throughout the study.

2.3 Thermal Injury by Laser Irradiation

Raft tissue was irradiated with one pulse from a perovskite (λ=1341 nm) laser (Dualis™, Fotona, Ljubljana, Slovenia). An ~2 mm diam spot was irradiated near the center of the raft using fluence of 20 J/cm² and pulse duration of 20 ms.

2.4 OCT

Broadband light from a superluminescent diode (10 mW with a center wavelength of 1310 nm) was coupled into a Michelson interferometer. A collinear visible source (633 nm) was employed for beam positioning on the raft. Backscattered light from the sample was combined with the reference to generate interference fringes on a photodetector. A rapid-scanning optical delay (RSOD) line was used for rapid axial scanning. Phase modulation of the signal was generated by an electro-optic phase modulator. The RSOD scanning rate and modulation frequency of the phase modulator were 400 Hz and 500 kHz, respectively. The image acquisition time was approximately 7 s and the number of data points for each A-line data acquisition was 4096. The lateral and axial resolutions were 10 and 15 μm, respectively.

2.5 MPM

Ultrafast pulses (150 fs, 800 nm) from a Ti:Al₂O₃ oscillator pumped by a frequency doubled Nd:YVO₄ laser were coupled into an inverted microscope. Galvanometer driven mirrors scanned the laser pulses in the focusing plane. Non-linear optical signals from the sample were collected by the focusing objective in backscatter geometry and directed to a photomultiplier tube (PMT) for photon counting detection. One of three filters was placed in front of the PMT for spectrally selective imaging. A 400 nm [10 nm, full width at half maximum (FWHM)] band pass filter was used to isolate SHG. A 520 nm (40 nm, FWHM) band pass filter was used to isolate fluorescence. A Schott colored glass filter which transmits 390–570 nm, FWHM, was used to image both SHG and fluorescence collectively. The acquisition rate for 256×256 pixel images was approximately 1 Hz with a pixel dwell time of ~20 μs.

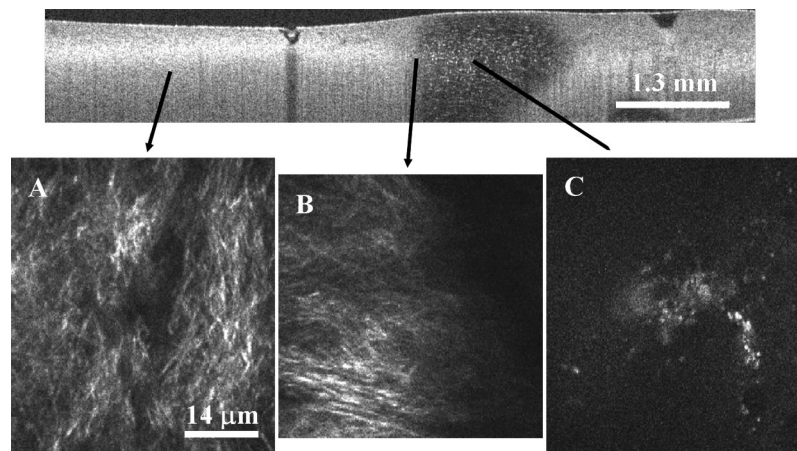


Fig. 3 OCT intensity image of the raft immediately after laser thermal injury with corresponding MPM images using SHG in collagen from (A) nonirradiated, (B) edge of laser irradiated, and (C) laser irradiated regions. The fluorescence in (C) is imaged through a Schott colored glass filter.

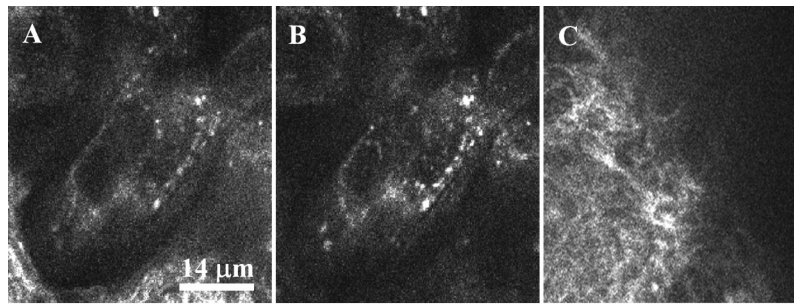


Fig. 4 Representative MPM images of the raft showing infiltration of fibroblast cells into the laser irradiated region two days after injury. (A) MPM image using cellular fluorescence and SHG in collagen. (B) A band pass filter at 520 nm was used to image cellular fluorescence. (C) A band pass filter at 400 nm was used to image SHG in collagen.

2.6 Histopathology

Raft specimens were examined immediately postirradiation and subsequently over three weeks. All samples were fixed for 24 h in buffered 10% formalin and then transferred to phosphate buffered saline. The samples were embedded in paraffin, cut into 6 μm thick sections, and mounted onto albumin-coated slides for hematoxylin and eosin (H&E) staining.

Three digital images were taken from each sample slide using an optical microscope (model BH-2, Olympus) and a digital camera (DP10, Olympus), and then standardized using computer software (Adobe Photoshop).

3 Results and Discussion

The engineered, *in vitro* skin-equivalent raft tissue models the dermis and epidermis using a collagen matrix embedded with human fibroblast cells and stratified epidermal layers from human keratinocytes. A H&E stained histopathology section of the raft is shown in Fig. 1 that has a dermal layer composed of collagen and fibroblast cells and stratified epidermis that shows approximately 10 layers with stratum corneum on the surface.

The effect of laser irradiation and subsequent raft wound healing response can be monitored using histopathology. Fig-

ure 2 shows H&E stained sections of control nonirradiated and irradiated regions of the raft immediately after laser irradiation and 10 days thereafter. The raft tissue in Figs. 2(A) and 2(B) shows a dense, fibrous collagen structure in the dermis and a stratified epidermis. The decrease in dermal thickness from day 1 to 10 is believed to be due to contraction mediated by fibroblast cells.¹⁶

The edge of the irradiated region is clearly delineated in Fig. 2(C). Vertical (horizontal) arrowheads point to the irradiated (nonirradiated) region in Figs. 2(C) and 2(D). The collagen fibrous structure is lost within the irradiated region [Fig. 2(E)]. Histopathology suggests that the thermal denaturation of collagen leads to increased dye uptake, resulting in a highly stained section. Fibroblast cells within the irradiated region are not viable as noted in Fig. 2(E). After 10 days, the irradiated region can still be delineated in Fig. 2(D) (vertical arrowhead) by the low density of collagen. The collagen matrix has reformed, but the dermis has not yet recovered completely compared to that in Fig. 2(B). Viable fibroblast cells can be seen within the irradiated region [Fig. 2(F)].

An OCT image of the raft immediately after laser irradiation is shown in Fig. 3 along with three high resolution MPM images. The OCT picture is a cross-sectional intensity image

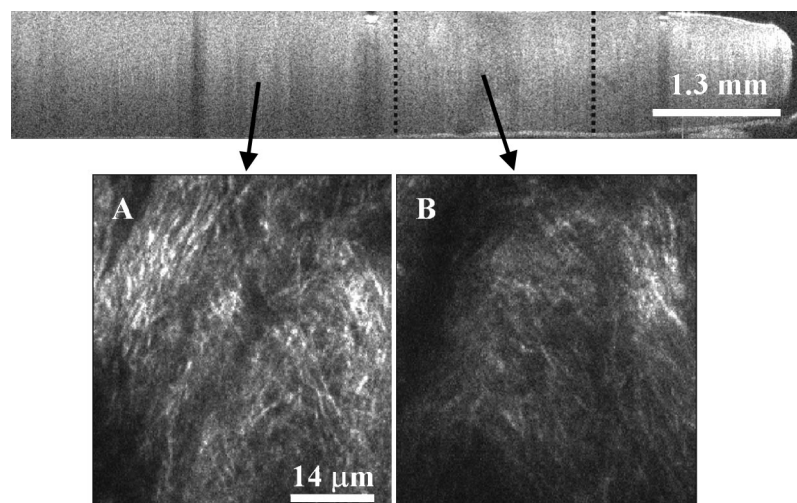


Fig. 5 OCT intensity image of the raft seven days after laser thermal injury with corresponding MPM images using SHG in collagen from the (A) nonirradiated and (B) laser irradiated regions. Recovery of the collagen matrix in (B) is incomplete.

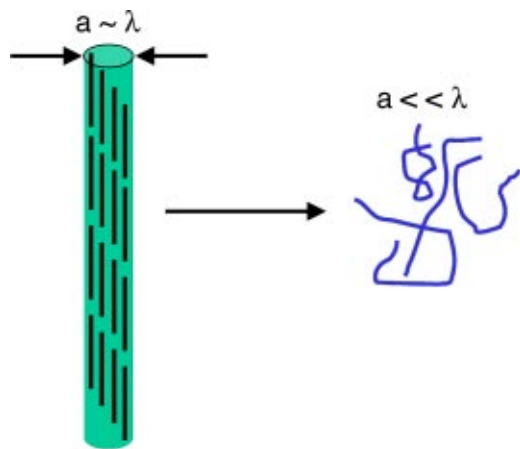


Fig. 6 Schematic of collagen thermal denaturation from an ordered array of molecules with a characteristic length comparable to the probe laser wavelength to randomly oriented collagen molecules with a characteristic length much less than the probe laser wavelength.

with a high (low) signal from the nonirradiated (irradiated) region. MPM images are shown from the nonirradiated [Fig. 3(A)], edge of the irradiated [Fig. 3(B)] and irradiated regions [Fig. 3(C)]. The MPM imaging plane is orthogonal to that of OCT (i.e., en face). SHG from collagen is used to image a dense fibrous matrix in the nonirradiated region of Fig. 3(A). A band pass filter at 400 nm was placed in front of the PMT to isolate the SHG signal. At the edge of the irradiated region, the sudden loss of SHG signal indicates the thermally damaged matrix as seen in Fig. 3(B). Within the irradiated region, there was no SHG signal except for in isolated regions of fluorescence presumably from cellular debris as shown in Fig. 3(C). Fluorescence was imaged by replacing the 400 nm band pass filter with a Schott colored glass filter.

Two days after laser irradiation, infiltration of the exposed region by fibroblast cells is observed by MPM as shown in Fig. 4. The MPM images are representative of fibroblast cells migrating into the thermally injured area and progressively remodeling the matrix predominantly from the edges inward.¹⁷ Figure 4(A) is characteristic of the wound healing response as fibroblast cells migrate towards the edge of the thermally injured region. The fibroblast cells are isolated in Fig. 4(B) by a band pass filter centered at 520 nm in front of the PMT. The filter was chosen to discriminate cellular fluorescence from pyridine nucleotides.¹⁸ SHG from collagen is shown in Fig. 4(C).

Seven days after laser irradiation, an OCT image shows recovery of raft light scattering from the irradiated region (delineated by black dotted lines; see Fig. 5). High resolution MPM images using SHG from collagen showed a reformed, fibrous matrix in the irradiated region [Fig. 5(B)] comparable to that in the control nonirradiated region [Fig. 5(A)]. However, matrix recovery is not complete in the irradiated region since imaging planes above and below Fig. 5(B) show regions of no signal, consistent with observations made by histopathology [Fig. 2(F)].

High contrast imaging of thermal injury in the raft observed by OCT and MPM is believed to be due to gross structural changes in collagen. The light scattering properties of human skin and organotypic, skin-equivalent tissues are pre-

dominantly determined by collagen and have been described as Mie scattering by cylinders of infinite length.⁷ Thermal denaturation of collagen reduces the characteristic length of the scatterer to much less than the wavelength of light (Rayleigh scattering), leading to reduced light scattering (see Fig. 6). This is evident in the OCT images shown in Fig. 3. Thermal denaturation results in the loss of collagen molecular organization which can have profound consequences on SHG.¹⁵ In the MPM images, the thermally injured region is indicated by the complete loss of SHG as seen in Fig. 3.

This study demonstrates the potential of OCT and MPM for burn depth determination and noninvasive serial monitoring of wound healing processes in human skin. Linear and nonlinear laser-tissue interactions were used to relate the collagen microstructure organization to bulk tissue optical properties. OCT was sensitive to tissue optical scattering which is believed to be primarily from collagen matrix components. High resolution MPM using SHG was shown to be highly dependent on the collagen molecular organization. Together, these measurements indicate that the thermal denaturation of collagen resulted in the reduction of tissue optical scattering and loss of SHG, leading to high contrast imaging of thermal injury. Intravital MPM imaging of fibroblast cell infiltration into the injured region provided insight into the raft wound healing processes. Simultaneous measurements of optical scattering and two-photon excited fluorescence have been reported previously to image the cell and tissue structure.¹⁹ Sequential measurements by OCT and MPM in this study further suggest simultaneous acquisition of nonlinear optical signals with the functionality of OCT^{20,21} would provide a powerful modality for imaging the function and structure of tissue.

Acknowledgments

This work was supported by the National Center for Research Resources of the National Institutes of Health (Laser Microbeam and Medical Program, RR-01192), the National Institutes of Health [AR-47551 to one of the authors (J.S.N.)], the U.S. Air Force Office of Scientific Research, Medical Free-Electron Laser (F49620-00-1-0371), and the Arnold and Mabel Beckman Foundation.

References

1. D. Huang, E. A. Swanson, C. P. Lin, J. S. Schuman, W. G. Stinson, W. Chang, M. R. Hee, T. Flotte, K. Gregory, and C. A. Puliato, "Optical coherence tomography," *Science* **254**, 1178–1181 (1991).
2. W. Denk, J. H. Strickler, and W. W. Webb, "Two-photon laser scanning fluorescence microscopy," *Science* **248**, 73–76 (1990).
3. E. Bell, H. P. Ehrlich, D. J. Buttle, and T. Nakatsuji, "Living tissue formed *in vitro* and accepted as skin-equivalent tissue of full thickness," *Science* **211**, 1052–1054 (1981).
4. A. El-Ghalbzouri, S. Gibbs, E. Lamme, C. A. Van Blitterswijk, and M. Ponc, "Effect of fibroblasts on epidermal regeneration," *Br. J. Dermatol.* **147**, 230–243 (2002).
5. A. Agarwal, M. L. Coleno, V. P. Wallace, W. Y. Wu, C. H. Sun, B. J. Tromberg, and S. C. George, "Two-photon laser scanning microscopy of epithelial cell-modulated collagen density in engineered human lung tissue," *Tissue Eng.* **7**, 191–202 (2001).
6. *Collagen*, edited by M. E. Nimni (Chemical Rubber, Boca Raton, FL, 1988).
7. I. S. Saidi, S. L. Jacques, and F. K. Tittel, "Mie and Rayleigh modeling of visible-light scattering in neonatal skin," *Appl. Opt.* **34**, 7410–7418 (1995).
8. B. H. Park, C. Saxer, S. M. Srinivas, J. S. Nelson, and J. F. de Boer,

- “*In vivo* burn depth determination by high-speed fiber-based polarization sensitive optical coherence tomography,” *J. Biomed. Opt.* **6**, 474–479 (2001).
9. J. F. de Boer, T. E. Milner, M. J. C. van Gemert, and J. S. Nelson, “Two-dimensional birefringence imaging in biological tissue by polarization-sensitive optical coherence tomography,” *Opt. Lett.* **22**, 934–936 (1997).
 10. A. T. Yeh, N. Nassif, A. Zoumi, and B. J. Tromberg, “Selective corneal imaging using combined second harmonic generation and two-photon excited fluorescence,” *Opt. Lett.* **27**, 2082–2084 (2002).
 11. P. J. Campagnola, A. C. Millard, M. Terasaki, P. E. Hoppe, C. J. Malone, and W. A. Mohler, “Three-dimensional high-resolution second-harmonic generation imaging of endogenous structural proteins in biological tissues,” *Biophys. J.* **81**, 493–508 (2002).
 12. R. M. Williams, W. R. Zipfel, and W. W. Webb, “Multiphoton microscopy in biological research,” *Curr. Opin. Chem. Biol.* **5**, 603–608 (2001).
 13. P. Stoller, B.-M. Kim, A. M. Rubenchik, K. M. Reiser, and L. B. Da Silva, “Polarization-dependent optical second-harmonic imaging of a rat-tail tendon,” *J. Biomed. Opt.* **7**, 205–214 (2002).
 14. P. Stoller, K. M. Reiser, P. M. Celliers, and A. M. Rubenchik, “Polarization-modulated second harmonic generation in collagen,” *Biophys. J.* **82**, 3330–3342 (2002).
 15. A. T. Yeh, B. Choi, J. S. Nelson, and B. J. Tromberg, “Reversible dissociation of collagen in tissues,” *J. Invest. Dermatol.* **121**, 1332–1335 (2003).
 16. E. Bell, B. Ivarsson, and C. Merrill, “Production of a tissue-like structure by contraction of collagen lattices by human fibroblasts of different proliferative potential *in vitro*,” *Proc. Natl. Acad. Sci. U.S.A.* **76**, 1274–1278 (1979).
 17. W. G. Jung, B. Kao, K. M. Kelly, J. S. Nelson, and Z. Chen, “Optical coherence tomography for *in vitro* monitoring of wound healing after laser irradiation,” *IEEE J. Sel. Top. Quantum Electron.* **9**, 222–226 (2003).
 18. S. Huang, A. A. Heikal, and W. W. Webb, “Two-photon fluorescence spectroscopy and microscopy of NAD(P)H and flavoprotein,” *Biophys. J.* **82**, 2811–2825 (2002).
 19. E. Beaurepaire, L. Moreaux, F. Amblard, and J. Mertz, “Combined scanning optical coherence and two-photon-excited fluorescence microscopy,” *Opt. Lett.* **24**, 969–971 (1999).
 20. Y. Zhao, Z. Chen, C. Saxer, S. Xiang, J. F. de Boer, and J. S. Nelson, “Phase-resolved optical coherence tomography and optical Doppler tomography for imaging blood flow in human skin with fast scanning speed and high velocity sensitivity,” *Opt. Lett.* **25**, 114–116 (2000).
 21. B. H. Park, M. C. Pierce, B. Cense, and J. F. de Boer, “Real-time multi-functional optical coherence tomography,” *Opt. Express* **11**, 782–793 (2003).